© 2018. Published by The Company of Biologists Ltd | Journal of Cell Science (2018) 131, jcs211342. doi:10.1242/jcs.211342

RESEARCH ARTICLE

Retromer associates with the cytoplasmic amino-terminus of polycystin-2

Frances C. Tilley[1], Matthew Gallon[1], Chong Luo[2,3], Chris M. Danson[1], Jing Zhou[2] and Peter J. Cullen[1,*]

ABSTRACT

Autosomal dominant polycystic kidney disease (ADPKD) is the most common monogenic human disease, with around 12.5 million people affected worldwide. ADPKD results from mutations in either *PKD1* or *PKD2*, which encode the atypical G-protein coupled receptor polycystin-1 (PC1) and the transient receptor potential channel polycystin-2 (PC2), respectively. Although altered intracellular trafficking of PC1 and PC2 is an underlying feature of ADPKD, the mechanisms which govern vesicular transport of the polycystins through the biosynthetic and endosomal membrane networks remain to be fully elucidated. Here, we describe an interaction between PC2 and retromer, a master controller for the sorting of integral membrane proteins through the endo-lysosomal network. We show that association of PC2 with retromer occurs via a region in the PC2 cytoplasmic amino-terminal domain, independently of the retromer-binding Wiskott-Aldrich syndrome and scar homologue (WASH) complex. Based on observations that retromer preferentially interacts with a trafficking population of PC2, and that ciliary levels of PC1 are reduced upon mutation of key residues required for retromer association in PC2, our data are consistent with the identification of PC2 as a retromer cargo protein.

This article has an associated First Person interview with the first author of the paper.

KEY WORDS: Endosome, Polycystin-2, Retromer

INTRODUCTION

Mutations in *PKD2*, which encodes the calcium-activated calcium channel polycystin-2 (PC2), underlie around 15% of autosomal dominant polycystic kidney disease (ADPKD) cases (Koulen et al., 2002; Rossetti et al., 2007; Zhou and Pollak, 2015). ADPKD affects between 1 in 500 and 1 in 4000 people worldwide, and is characterised by the formation of multiple bilateral renal cysts, which have devastating consequences on organ function (Torres et al., 2007). PC2 is predominantly localised to the endoplasmic reticulum (ER), but is also found in the primary cilia of renal tubule epithelia in association with polycystin-1 (PC1) (Koulen et al., 2002; Yoder et al., 2002; Nauli et al., 2003). Here, the polycystin complex functions to modulate a wide variety of intracellular signalling pathways, including canonical and non-canonical Wnt signalling, cyclic adenosine monophosphate, G-protein coupled receptor (GPCR) and mammalian target of rapamycin pathways (Nauli et al., 2006; Zhou, 2009; Chapin and Caplan, 2010; Fedeles et al., 2014).

The absence of either polycystin protein from the primary cilium is sufficient to promote kidney cystogenesis, and a number of *PKD1* and *PKD2* mutants that are defective in ciliary trafficking are reported to be pathogenic (Ma et al., 2013; Cai et al., 2014; Su et al., 2015). Several studies have therefore addressed the question of how PC1 and PC2 traffic to the primary cilium from compartments of the biosynthetic membrane trafficking network, with roles for PC1-PC2 complex formation, cleavage of PC1 at a juxtamembrane GPCR autoproteolytic site, VxP ciliary targeting motifs, an internal PLAT domain in PC1 and Rabep1-GGA1-Arl3, BBSome and exocyst trafficking modules having all been implicated (Hanaoka et al., 2000; Geng et al., 2006; Kim et al., 2014; Fogelgren et al., 2011; Su et al., 2014; Su et al., 2015; Xu et al., 2016).

Many of the trafficking proteins involved in both ciliogenesis and the delivery of ciliary-resident proteins to this organelle were first experimentally associated with canonical vesicular trafficking pathways (Sung and Leroux, 2013). Exocyst, for example, was initially characterised as being required for the vesicular transport of cargo proteins from the Golgi complex to the plasma membrane in yeast (Novick et al., 1980; TerBush et al., 1996). Members of the Eps15 homology domain (EHD) protein family, which have roles in early stages of ciliogenesis, have long been known to function in membrane remodelling processes within the endosomal network (Naslavsky and Caplan, 2011; Lu et al., 2015; Bhattacharyya et al., 2016). Additionally, a recent study has demonstrated localisation of the endosomal protein serologically defined colon cancer antigen-3 (SDCCAG3) to the basal body of primary cilia, and implicated its activity in ciliary targeting of PC2 (Yu et al., 2016).

The concept that components of the endosomal trafficking network have been co-opted by cells in order to sustain normal cilia function is supported by a recent study in which stable isotope labelling with amino acids in culture (SILAC)-based quantitative proteomics of the retromer complex revealed PC2 as a putative interaction partner (McMillan et al., 2016). Comprising subunits VPS35, VPS29 and either VPS26A or VPS26B, retromer is an evolutionarily conserved heterotrimer which functions at the endosome membrane to promote the retrieval of transmembrane proteins, or 'cargo', away from a degradative fate in the lysosome (Seaman et al., 1998; Koumandou et al., 2011; Gallon and Cullen, 2015). The absence of retromer is thus correlated with increased lysosomal targeting of protein cargo, and is exemplified by the loss of the glucose transporter GLUT1 and the β2-adrenergic receptor (β2-AR) that occurs upon VPS35 knockdown (Temkin et al., 2011; Steinberg et al., 2013). Retromer was initially described as a cargo-selective complex, but it also serves an additional function as a molecular scaffold (Seaman et al., 1998; Nothwehr et al., 1999; Seaman, 2004; Harbour et al., 2010; Fjorback et al., 2012). That is, retromer recruits and co-ordinates the activity of a variety of proteins to regulate cargo selection, the formation of intermediate tubular and vesicular recycling carriers, Rab guanosine

[1]School of Biochemistry, Biomedical Sciences Building, University of Bristol, Bristol BS8 1TD, UK. [2]Harvard Center for Polycystic Kidney Disease Research and Renal Division, Department of Medicine, Brigham and Women's Hospital, Harvard Medical School, Boston, MA 02115, USA. [3]Kidney Disease Center, First Affiliated Hospital, School of Medicine, Zhejiang University, Hangzhou 310058, People's Republic of China.

*Author for correspondence (pete.cullen@bristol.ac.uk)

F.C.T., 0000-0002-6021-4989; P.J.C., 0000-0002-9070-8349

Received 21 September 2017; Accepted 26 April 2018

Journal of Cell Science (2018) 131, jcs211342. doi:10.1242/jcs.211342

triphosphatase (GTPase) cycling and cytoskeletal dynamics (Harbour et al., 2010; Gallon and Cullen, 2015).

In this study, we present work validating the putative interaction between PC2 and retromer, and identify a motif in the amino (N)-terminal domain of PC2 required for retromer association. We find that localisation of a PC2 N-terminal peptide to VPS35-positive endosomes is perturbed upon mutation of this motif, although interaction between full-length PC2 and retromer appears to depend on multivalent interactions. Our data show that exogenous PC2 preferentially interacts with retromer either when the carboxy (C)-terminal domain of PC2, containing both an ER-retention signal and a PC1 binding site, is truncated, or when co-expressed with PC1, suggesting that retromer associates with a trafficking population of PC2. In addition, we find that the PC1 ciliary trafficking defect associated with knockout of *PKD2* in mouse kidney tubule epithelial cells is not rescued to the same extent with reintroduction of PC2 bearing mutations in the motif required for association with retromer as it is upon transfection of wild-type PC2.

RESULTS

PC2 associates with the retromer complex via its cytoplasmic N-terminus

PC2 was originally identified as a putative retromer-interacting protein in a mass-spectrometry-based study, in which SILAC-based proteomics were employed to establish a retromer interactome (McMillan et al., 2016). To confirm the association of retromer with PC2, RPE-1 cells lentivirally expressing either GFP-VPS26A, GFP-VPS26B, GFP-VPS29 or GFP-VPS35 were subjected to GFP-nanotrap immunoisolation (GFP-trap) followed by western analysis. Endogenous PC2 was immunoprecipitated, to some extent, by all retromer subunits (Fig. 1A). FAM21 and SNX27 were also immunoprecipitated by retromer components, serving as a positive control in these experiments (Jia et al., 2012; Steinberg et al., 2013; Lee et al., 2016).

PC2 possesses both N- and C-terminal cytoplasmic domains, which we took to be the primary candidate regions in PC2 for mediating the interaction with retromer. Immunoprecipitation of GFP-tagged N- and C-terminal PC2 fragments, comprising residues 1-223 [PC2(1-223)-GFP] and 680-968 [PC2(680-968)-GFP], respectively, from HEK293T cells revealed that retromer components VPS35, VPS26A and VPS26B only associate with the PC2 N-terminal domain (Fig. 1B). Consistent with this finding, we observed colocalisation of PC2(1-223)-GFP with sorting nexin-1 (SNX1) a protein that localises to the same endosomal compartment as retromer (Rojas et al., 2007), and a concordant decrease in the Pearson's correlation coefficient (PCC) of PC2(1-223)-GFP and SNX1 following knockdown of VPS35 (Fig. 1Ci-iii).

Identification of a retromer association motif in the PC2 N-terminus

The PC2 N-terminal domain does not contain any established retromer-binding motifs, such as, for example, the Trp-Leu-Met (WLM) and FANSHY motifs reported to mediate the endosome to *trans*-Golgi network recycling of the cation-independent mannose-6-phosphate receptor (CI-MPR) and sorting protein-related receptor with A-type repeats (SORLA), respectively (Seaman, 2004; Fjorback et al., 2012). Nor does the PC2 N-terminus contain a recognisable post-synaptic density-95/discs large/zona occuldens-1 (PDZ)-binding motif, required for the retromer-mediated endosome-to-plasma membrane recycling of transmembrane proteins containing a PDZ-binding motif, via interaction with the SNX27 cargo adaptor (Temkin et al., 2011; Steinberg et al., 2013; Lee et al., 2016).

The PC2 N-terminus does contain an evolutionarily conserved $R^{6}VxP^{9}$ motif, which has been linked to the trafficking of PC2 from compartments of the biosynthetic pathway to the primary cilium (Geng et al., 2006). In order to determine whether PC2 was interacting with retromer via this motif, we used site-directed mutagenesis to generate the point mutations p.R6G, p.V7A and p.P9A in PC2(1-223)-GFP. However, we found that these mutant PC2 peptides were able to immunoprecipitate retromer components to the same extent as the wild-type PC2 N-terminal domain (Fig. 2A).

In order to identify the region within the PC2 N-terminal domain required for association with retromer, we created a series of truncated PC2 constructs by subcloning the regions encoding residues 1-48, 1-60, 1-70, 1-84, 1-94 and 1-156 into the pEGFP-N1 vector, which encodes a C-terminal GFP-tag. Immunoprecipitation of these truncated PC2 peptides from HEK293T cells, followed by western analysis, revealed that all constructs displayed the ability to immunoprecipitate retromer with the exception of PC2(1-48)-GFP (Fig. 2Bi,ii), suggesting that the motif in PC2 required for retromer association is contained between residues Glu48 and Arg60. Alignment of the PC2 N-terminal domain protein sequence from different species revealed that although this region is reasonably well conserved in mammals, there is little sequence similarity between the *Homo sapiens* PC2 N-terminal domain and that in *Gallus gallus* and *Danio rerio* (Fig. 2C), and the same region in *Drosophila melanogaster* and *Caenorhabditis elegans* is markedly divergent (data not shown).

In order to determine which amino acids within this region are critical for association of PC2 with retromer, we used site-directed mutagenesis to sequentially mutate each amino acid between residues Glu48 and Arg60 in PC2(1-223)-GFP to an alanine (Fig. 3A). These mutant constructs were transiently transfected into HEK293T cells, and assessed for their ability to associate with VPS35 and VPS26A by GFP-trap and western analysis. We observed a variable effect of these mutations on the ability of the PC2 N-terminal fragment to immunoprecipitate retromer components, but consistently found that introduction of a p.I54A, p.E55A, p.M56A or p.I59A mutation almost completely abrogated the association of PC2(1-223)-GFP with VPS35 and VPS26A (Fig. 3Bi-iv). Concomitantly, in comparison to the punctate localization of the wild-type PC2 N-terminal domain when transiently expressed in HeLa cells, PC2(1-223)-GFP constructs bearing the p.I54A, p.M56A and p.I59A mutations all displayed a much more diffuse expression pattern, and exhibited a significantly reduced PCC with endogenous VPS35 compared to the wild-type PC2 N-terminus. In this experiment, cells expressing the PC2 C-terminal fragment PC2(680-968)-GFP were included as a negative control and a clear difference in the localisation pattern of this domain of PC2 compared with the N-terminal domain was observed, with no puncta visible and a drastically reduced PCC with endogenous VPS35 (Fig. 4A,B). Taken together, these data indicate that the PC2 N-terminal domain contains a linear motif with the sequence [G-x-x-I-E-M-Q-x-I-x] (where x is any amino acid), required for association with retromer.

The association of PC2 with retromer appears to depend on multivalent interactions

In order to determine whether the interaction between PC2 and retromer was occurring directly, we performed direct binding assays using recombinant PC2(1-223)-6×His, and GST-tagged retromer components VPS26A-myc, VPS35 and VPS29-myc (Fig. S1A). However, purified retromer components were unable to bind PC2(1-223)-6×His, and in the reverse direction, PC2(1-223)-6×His was

Journal of Cell Science (2018) 131, jcs211342. doi:10.1242/jcs.211342

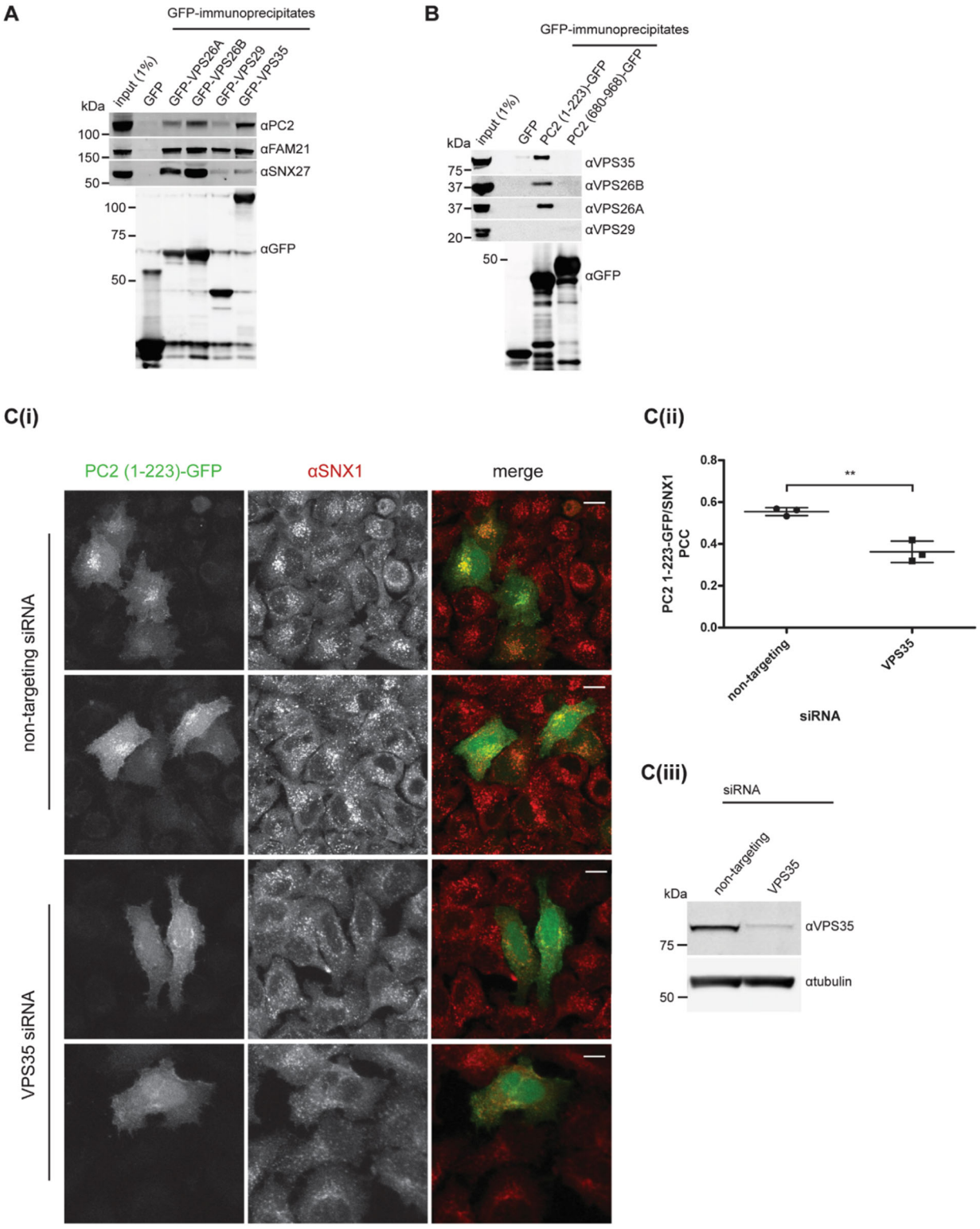

Fig. 1. PC2 associates with retromer via its cytoplasmic N-terminus. (A) RPE-1 cells lentivirally expressing GFP or GFP-tagged retromer components VPS26A, VPS26B, VPS29 or VPS35 were subjected to GFP-trap. The immunoprecipitates were then resolved by SDS-PAGE and immunoblotted with the indicated antibodies. (B) HEK293T cells were transiently transfected with a GFP-tagged PC2 N-terminal fragment (1-223), a GFP-tagged C-terminal fragment (680-968) or an empty GFP vector as a negative control. Cells were then subjected to GFP-trap followed by western analysis to determine association of the PC2 N- and C-terminal domains with retromer. A and B show single experiments which are representative of at least three independent biological repeats. (Ci) Fluorescence imaging of PC2(1-223)-GFP localisation in VPS35-suppressed and non-targeting siRNA-treated HeLa cells stained for endogenous SNX1. Scale bars: 10 µm. (ii) Quantification of PC2(1-223)-GFP and SNX1 colocalisation using Pearson's correlation coefficient (PCC) in VPS35-suppressed and non-targeting siRNA treated HeLa cells. Graph shows the mean PCC from three independent biological repeats, in which at least 20 cells per condition were analysed. Error bars are mean±s.d., $^{**}P<0.01$ determined using an unpaired two-tailed Student's *t*-test. (iii) Western blot showing representative levels of VPS35 protein in HeLa cells following transfection with a mixture of two siRNA oligos directed against VPS35, and a non-targeting control siRNA.

Journal of Cell Science (2018) 131, jcs211342. doi:10.1242/jcs.211342

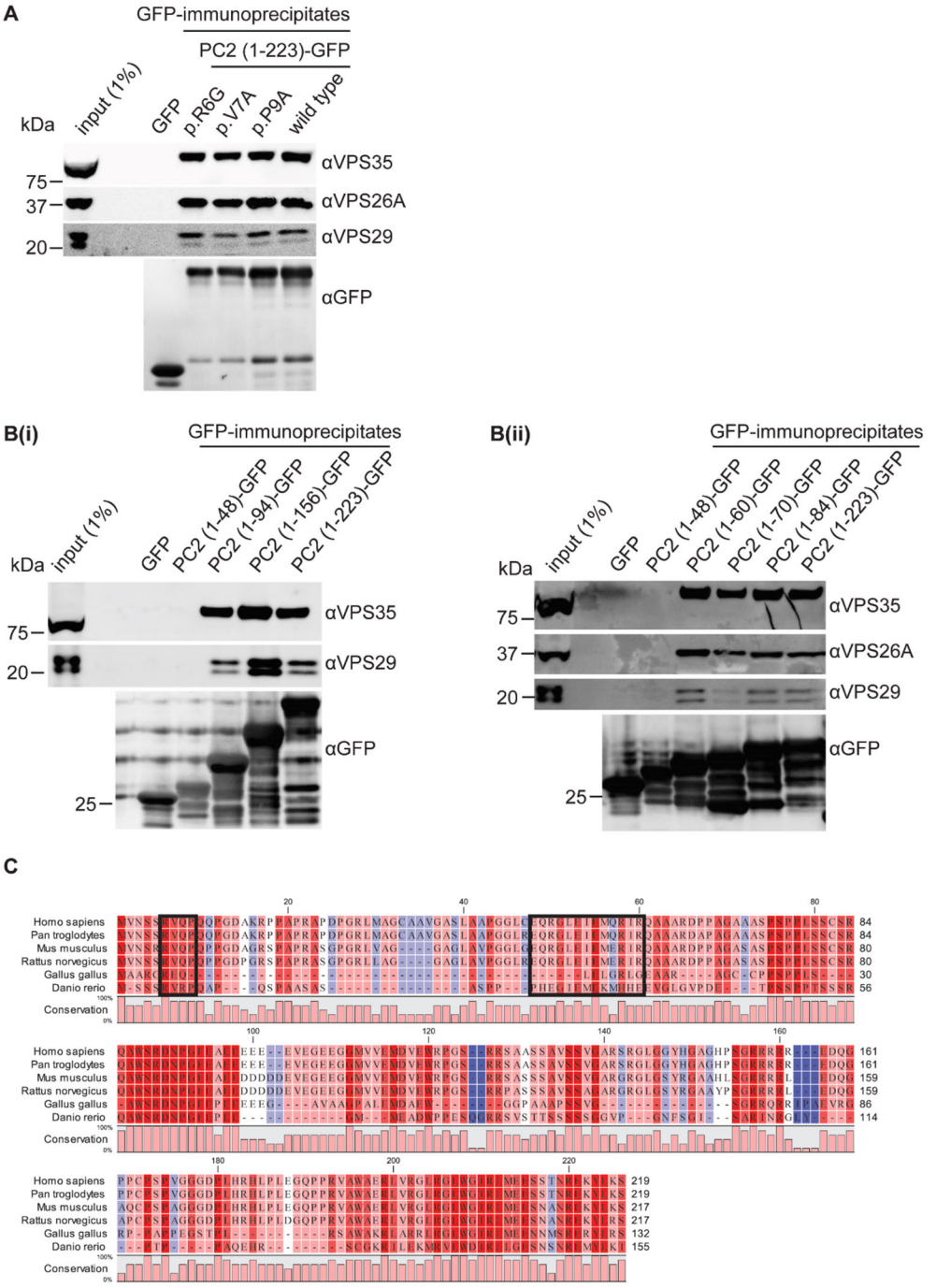

Fig. 2. PC2 associates with retromer independently of the $R^6V\times P^9$ motif, between residues Glu-48 and Arg-60. (A) HEK293T cells were transiently transfected with either a wild-type PC2 N-terminal fragment, or PC2(1-223)-GFP constructs bearing point mutations in the R^6VxP^9 motif (p.R6A, p.V7A and p.P9A). Cells were then subjected to GFP-trap followed by SDS-PAGE and immunoblotting with the indicated antibodies. (Bi,ii) HEK293T cells transfected with the indicated GFP-tagged PC2 amino-terminal truncation mutants subjected to GFP-trap followed by SDS-PAGE and immunoblotting to assess the ability of the various N-terminal PC2 fragments to immunoprecipitate retromer. (C) Alignment of the PC2 N-terminal cytoplasmic domain in the indicated species. The intensity of red colour is representative of the level of conservation of each residue among the indicated species, with blue marking the less conserved residues. Both the R^6VxP^9 motif and region required for associated with retromer are highlighted. A shows a single experiment that is representative of at least three independent repeats. Bi,ii show single experiments that are representative of 2 (i) or 3 (ii) independent biological repeats.

unable to bind GST-VPS26A-myc, GST-VPS35 or GST-VPS29-myc (Fig. S1B). We therefore hypothesised that the interaction of PC2 with retromer was occurring indirectly, perhaps via the retromer-associated Wiskott-Aldrich syndrome and scar homologue (WASH) complex, components of which are also enriched within the core retromer interactome (McMillan et al., 2016).

To investigate the possibility of an association between PC2 and the WASH complex, we transiently transfected HEK293T cells with both full-length YFP-tagged FAM21, and a GFP-tagged FAM21 'head' domain, which comprises amino acids 1-356, then performed GFP-trap and western analysis (Fig. 5A). Since retromer binds the C-terminal tail of FAM21 (Jia et al., 2012), the VPS26 subunit is only immunoprecipitated by full-length FAM21. The FAM21 'head' integrates into the rest of the WASH complex, and so strumpellin immunoprecipitates with both full-length and truncated FAM21. SNX27 exhibits the same pattern of immunoprecipitation as strumpellin, since in addition to directly binding the VPS26 retromer subunits, SNX27 is capable of retromer-independent binding to FAM21 (Steinberg et al., 2013; Lee et al., 2016). That we observed immunoprecipitation of PC2 with both the full-length and FAM21 'head' constructs suggests that PC2 is capable of independently interacting with both retromer and the WASH complex, in a manner analogous to SNX27. Alternatively, the interaction of PC2 with retromer may be occurring indirectly via FAM21, or an additional WASH complex component.

Journal of Cell Science (2018) 131, jcs211342. doi:10.1242/jcs.211342

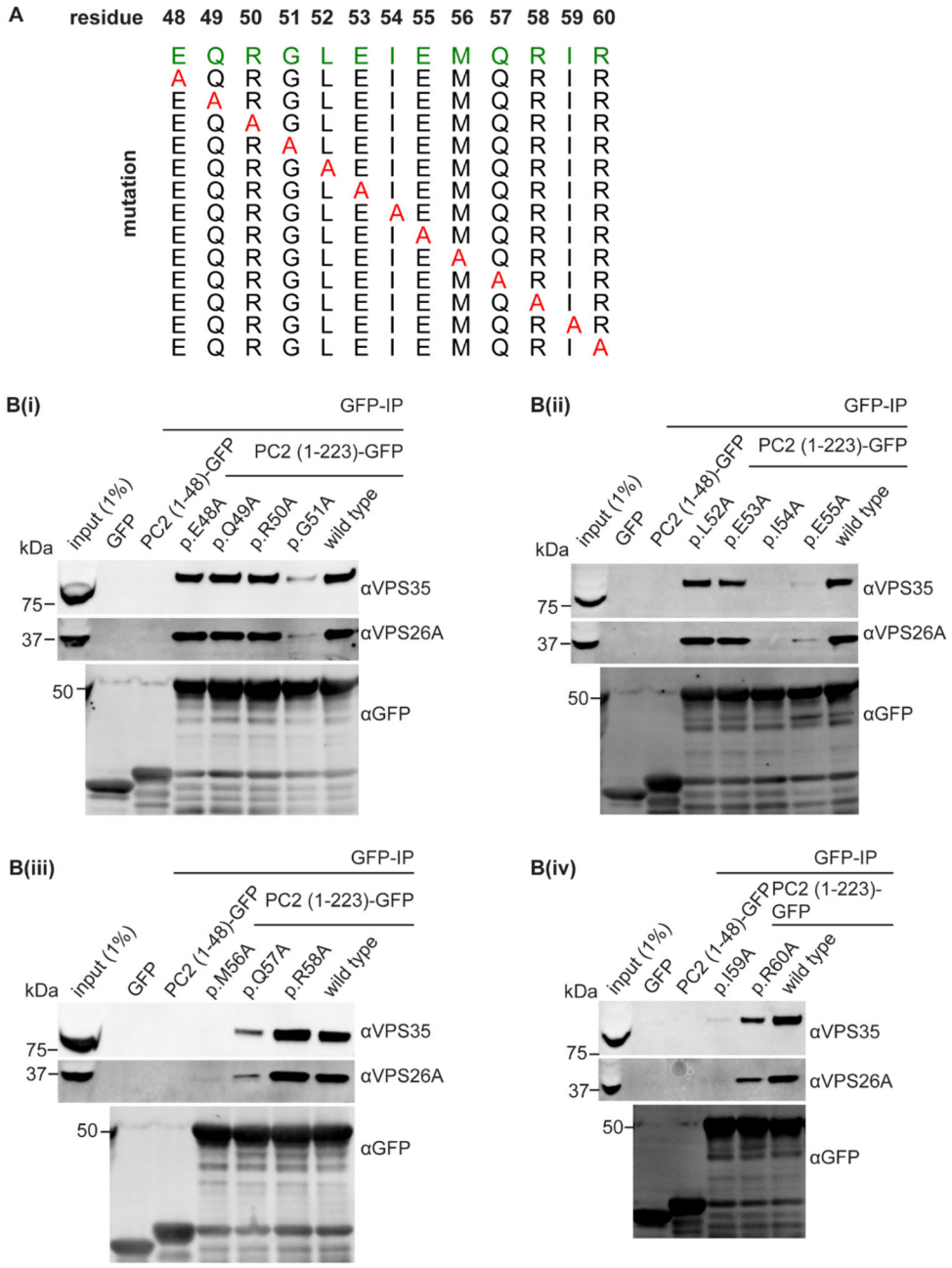

Fig. 3. Identification of the motif in PC2 required for retromer association. (A) Schematic representation of the array of mutations introduced into PC2(1-223)-GFP by site-directed mutagenesis in order to determine the residues required for association of PC2 with retromer. (Bi-iv) HEK293T cells were transfected with GFP-tagged PC2 N-terminal domain constructs bearing the point mutations outlined in A. Cells were also transfected with either an empty GFP-tagged vector, PC2 (1-48)-GFP or PC2(1-223)-GFP, which were included as negative and positive controls, respectively. Cells were then subjected to GFP-trap and western analysis to assess the ability of each construct to associate with VPS35 and VPS26A. Data show single experiments that are each representative of at least three independent biological repeats.

To test the latter hypothesis, we suppressed FAM21 using siRNA in RPE-1 cells lentivirally expressing GFP-VPS35, and then assessed the ability of GFP-VPS35 to immunoprecipitate PC2 in both FAM21-depleted and control conditions. As it is the interaction of the FAM21 with VPS35 that is argued to promote endosomal recruitment of the entire WASH complex (Harbour et al., 2012), suppression of FAM21 would decrease the availability of every WASH complex component at the endosome membrane. In these experiments, however, suppression of FAM21 had no effect on the ability of GFP-VPS35 to immunoprecipitate PC2 (Fig. 5B). Similarly, FAM21 suppression had no effect on the localisation of PC2(1-223)-GFP to VPS35-marked endosomes (Fig. 5Ci-iii). Together, these results indicate that the N-terminus of PC2 is not capable of interacting with the VPS35, VPS26A or VPS29 retromer subunits in isolation. However, if PC2 is binding retromer indirectly, this is not occurring in a manner dependent on interaction of retromer with the WASH complex.

Preferential interaction of retromer with C-terminal truncated PC2 and PC2-PC1 complexes

We have established that introduction of a p.I59A mutation abrogates the ability of PC2(1-223)-GFP to associate with VPS35 and VPS26A. However, when investigating the effect of this mutation on the localisation and interaction capabilities of full-length PC2, we found that we were unable to immunoprecipitate detectable amounts of retromer even with wild-type PC2 (Fig. 6A). We hypothesised that the inability of exogenous full-length PC2 to immunoprecipitate retromer components was a consequence of the localisation of this construct. Localisation of PC2 to the ER is thought to depend on phosphorylation of Ser812 by casein kinase-2 (CK2). This modification has been reported to allow recognition of PC2 by phosphofurin acidic cluster sorting protein-2 (PACS-2), an interaction which then promotes PC2 ER-Golgi translocation (Köttgen et al., 2005). Exit of PC2 from compartments of the biosynthetic

Journal of Cell Science (2018) 131, jcs211342. doi:10.1242/jcs.211342

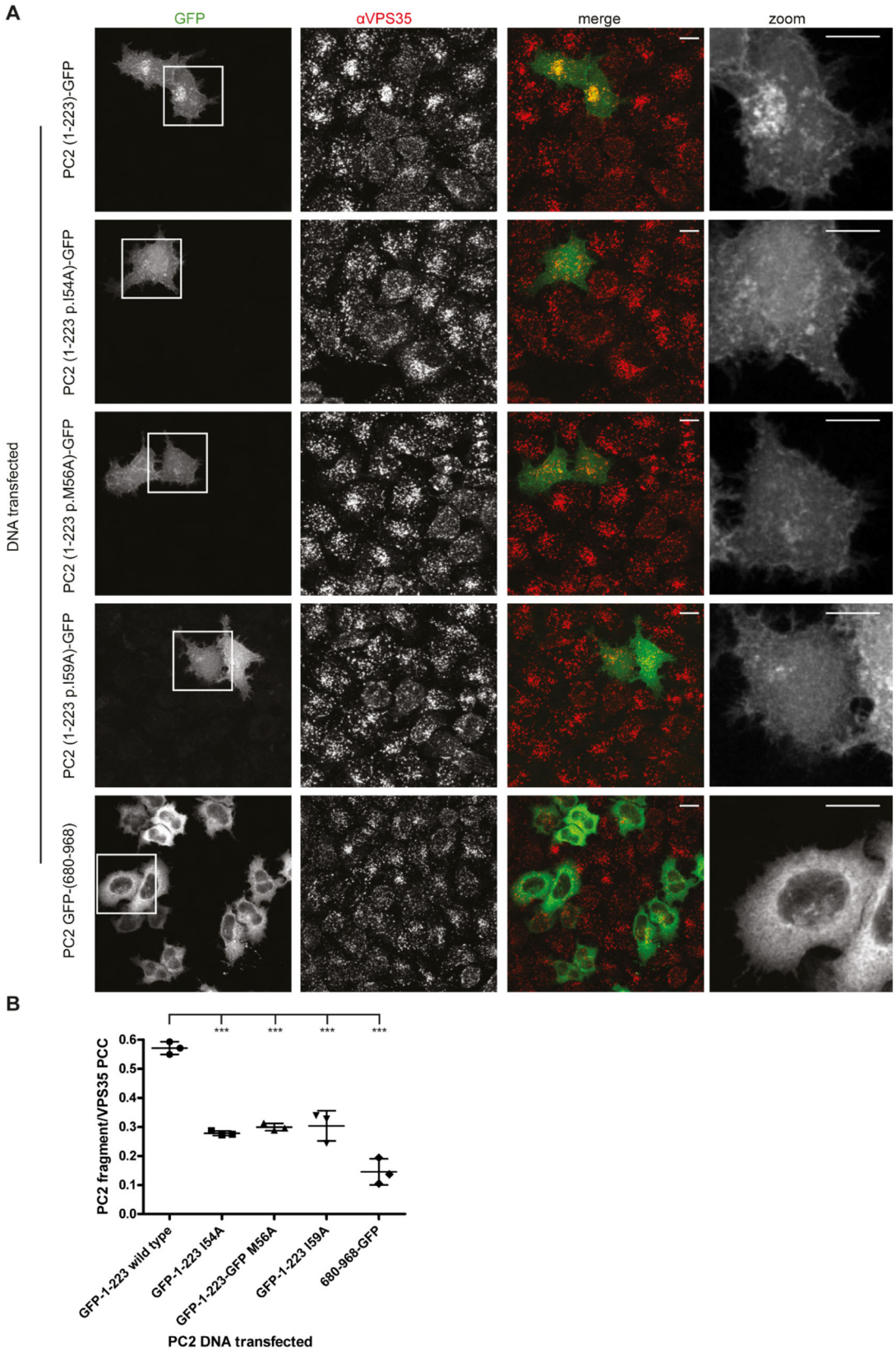

Fig. 4. PC2 N-terminal peptides bearing mutations in the retromer-association motif exhibit decreased endosomal localisation. (A) HeLa cells transiently expressing wild-type PC2(1-223)-GFP, PC2(1-223)-GFP bearing the point mutations p.I54A, p.M56A and p.I59A, and PC2(680-968)-GFP were fixed and stained for endogenous VPS35. Zoom panel shows enlargement of boxed area in GFP panel. Scale bars: 10 µm. (B) Quantification of colocalisation of each GFP-tagged PC2 peptide with endogenous VPS35 using PCC. The graph shows the mean PCC from three independent biological repeats in which at least 20 cells per condition were analysed. Error bars are mean±s.d., ***P<0.005 determined using the multiple comparisons function within the ordinary one-way ANOVA statistical test, followed by a Dunnett *post hoc* test, compared with PC2(1-223)-GFP control.

Journal of Cell Science (2018) 131, jcs211342. doi:10.1242/jcs.211342

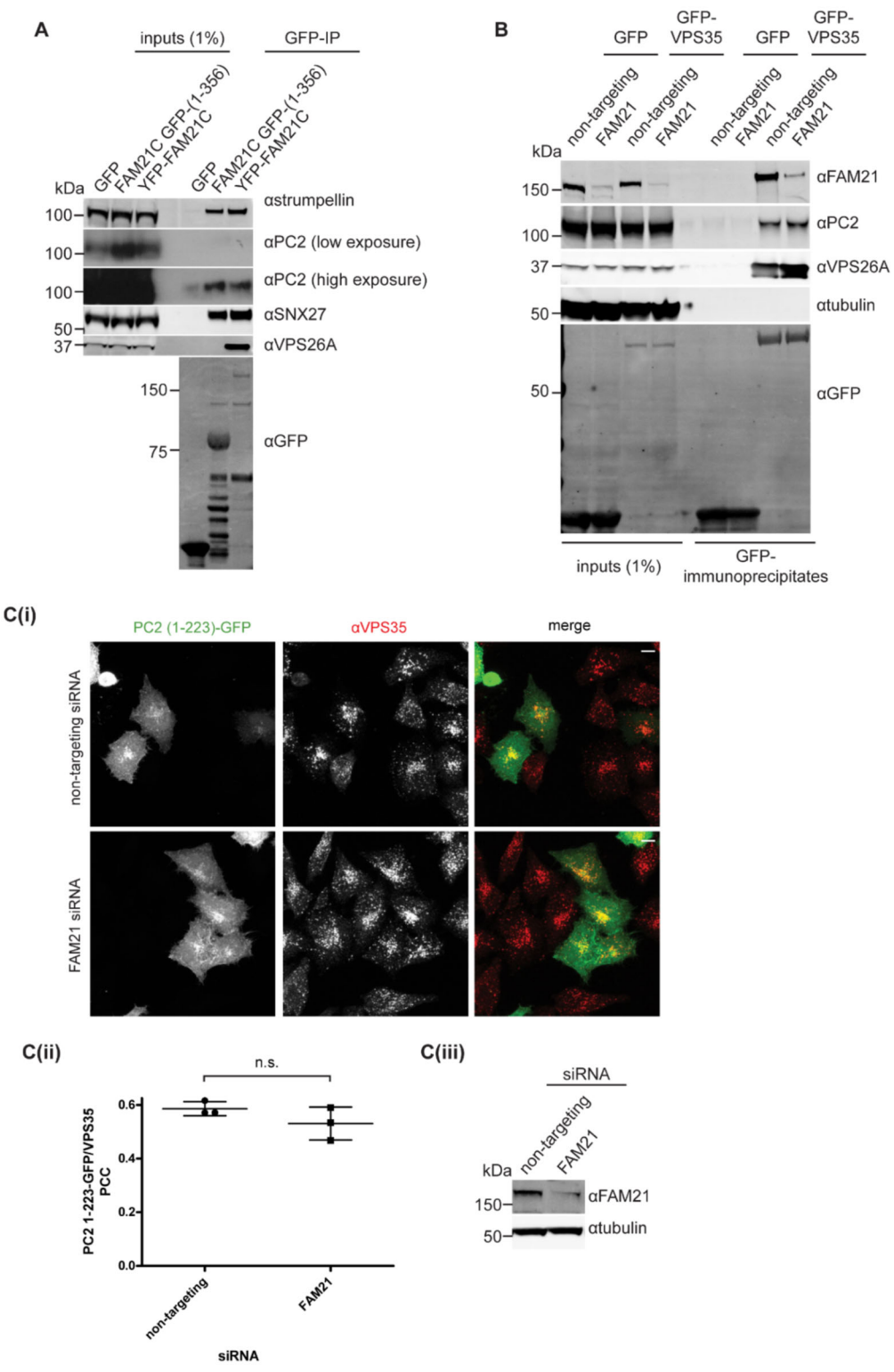

Fig. 5. PC2 is capable of independent interaction with the retromer-associated WASH complex. (A) HEK293T cells were transfected with the indicated FAM21 constructs, or an empty GFP vector as a negative control. Cells were then subjected to GFP-trap followed by western analysis in order to assess the ability of each construct to associate with strumpellin, PC2, SNX27 and VPS26A. (B) RPE-1 cells lentivirally expressing GFP or GFP-VPS35 were twice transfected with siRNA targeting FAM21, or non-targeting control siRNA. Cells were then subjected to GFP-trap followed by western blot analysis to determine association of VPS35 with VPS26A, PC2 and FAM21. A and B are representative of 2 (A) or 3 (B) independent biological repeats. (Ci) Fluorescence imaging of PC2(1-223)-GFP localisation in FAM21-suppressed and control siRNA treated HeLa cells stained for endogenous VPS35. Scale bars: 10 µm. (Cii) Quantification of PC2(1-223)-GFP and VPS35 colocalisation using PCC in VPS35-suppressed and non-targeting siRNA-treated control HeLa cells. Graph shows the PCC from three independent biological repeats, in which at least 25 cells per condition were analysed. Error bars are mean±s.d., with n.s. indicating that the difference between conditions is not significant as determined using an unpaired two-tailed Student's *t*-test. (Ciii) Western blot showing representative levels of FAM21 protein in HeLa cells following transfection with a mixture of four siRNA oligonucleotides directed against FAM21, and a non-targeting control siRNA.

membrane-trafficking network then depends on PC2 binding to proteins, such as PC1, which associate with its C-terminal domain and either mask, or create steric hindrance around, the ER-retention site contained there (Kim et al., 2014). Perhaps the rate-limiting availability of PC2 C-terminal-interacting proteins results in inefficient entry of exogenously expressed PC2 into the endosomal network, hence a reduced level of association with retromer. We therefore created a GFP-tagged C-terminally truncated PC2 protein that lacks both the CK2 phosphorylation site and the PC1-interacting domain located between PC2 residues 798 and 927, PC2(1-703)-GFP (Casuscelli et al., 2009). We found that PC2(1-703)-GFP was consistently able to immunoprecipitate a small amount of VPS35, and in contrast to full-length mPC2-GFP, localisation of PC2(1-703)-GFP was predominantly vesicular, colocalising extensively with endogenous VPS35 (Fig. 6B,C). We were also able to visualise co-trafficking of PC2(1-703)-GFP and mCherry-SNX1 in live HeLa cells

Journal of Cell Science (2018) 131, jcs211342. doi:10.1242/jcs.211342

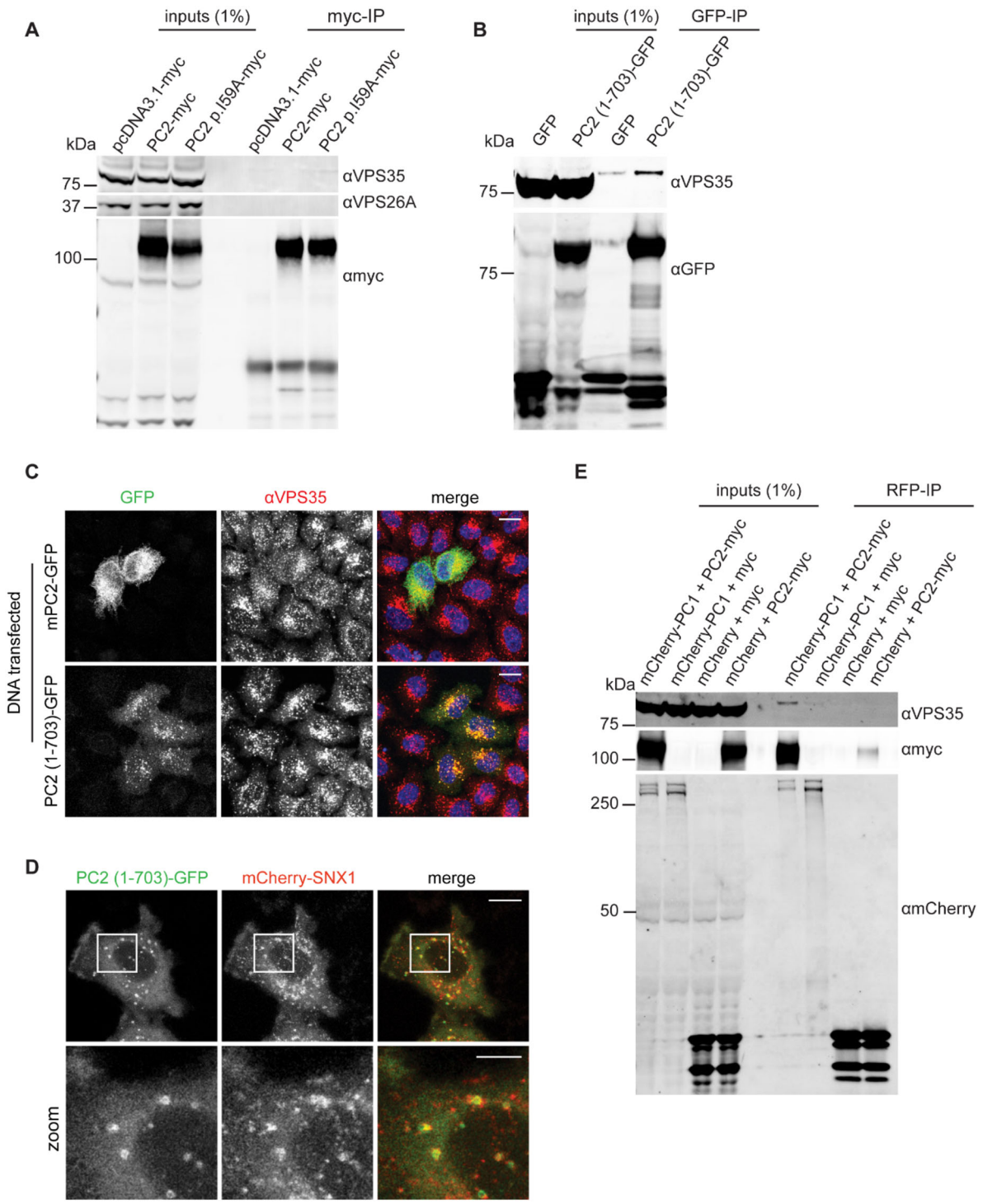

Fig. 6. Retromer preferentially interacts with a trafficking population of exogenous PC2. (A) HEK293T cells were transfected with either full-length wild-type PC2-myc, or a full-length PC2-myc construct bearing a p.I59A mutation. Cells were also transfected with an empty myc vector as a control. Cells were then subjected to myc immunoisolation, followed by western blot analysis to determine association of each construct with VPS35 and VPS26A. (B) HEK293T cells were transfected with PC2(1-703)-GFP, or an empty GFP vector as a negative control. Cells were then subjected to GFP-trap followed by western blot analysis, to determine the association of each construct with VPS35. (C) Fluorescence imaging of HeLa cells expressing either a full-length C-terminal GFP-tagged mPC2 construct, or PC2(1-703)-GFP. (D) Still from fluorescence live imaging of HeLa cells transiently transfected with both PC2(1-703)-GFP and mCherry-SNX1. Zoom panel shows enlargement of boxed area in top panel. Scale bars:10 µm (top) and 5 µm (bottom). (E) HEK293T cells were transfected with the indicated constructs (combinations of mCherry-PC1, empty mCherry, PC2-myc and empty myc). Cells were then subjected to RFP-trap followed western blot analysis to assess association of each construct with VPS35. All data in this figure are representative of either three (A,B,D,E) or two (C) independent biological repeats.

(Fig. 6D). In addition, we found we were able to immunoprecipitate a small amount of VPS35 from cells overexpressing both PC1 and PC2, but not from cells overexpressing either polycystin protein in isolation (Fig. 6E). These results suggest that retromer may preferentially interact with PC2 that has exited the ER and entered the endosomal trafficking network.

Journal of Cell Science (2018) 131, jcs211342. doi:10.1242/jcs.211342

Investigation into the functional relevance of the PC2-retromer interaction

Our results suggest that retromer is interacting with an endosomal trafficking population of PC2, implying either that PC2 is a retromer cargo molecule, or that PC2 may have some role in the regulation of vesicular recycling, which it exerts at the endosome membrane. If PC2 regulates retromer function, we might expect PC2 knockdown to phenocopy VPS35 suppression in a GLUT1 trafficking assay. However, we found that in contrast to VPS35-depleted conditions, in which GLUT1 becomes increasingly colocalised with the lysosomal marker LAMP1 due to defective endosome-to-plasma membrane recycling (Steinberg et al., 2013), the PCC of GLUT1 and LAMP1 in PC2-suppressed cells was not significantly increased compared with the PCC of GLUT1 and LAMP1 in control siRNA-transfected cells (Fig. 7A,B). This result indicates that PC2 does not affect the ability of retromer to participate in endosome-to-plasma membrane recycling of GLUT1, but does not necessarily rule out the possibility of a regulatory role for PC2 within the endosomal network, as will be discussed below.

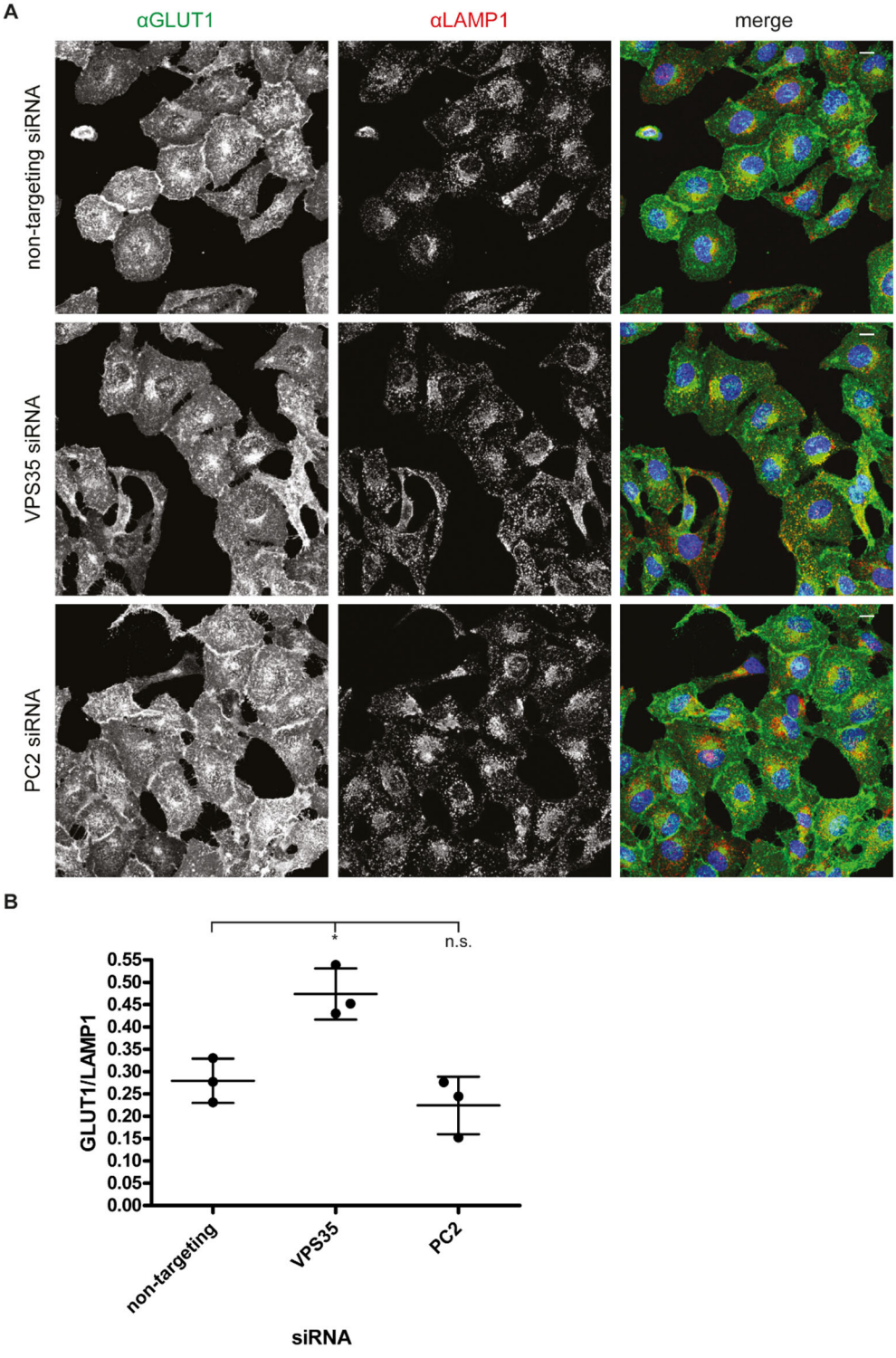

Fig. 7. PC2 does not affect the ability of retromer to recycle GLUT1. (A) VPS35 suppressed, PC2 suppressed and non-targeted siRNA-treated HeLa cells were stained for endogenous GLUT1 and LAMP1. Scale bars: 10 µm. (B) Colocalisation of GLUT1 and LAMP1 in each condition was determined using Pearson's correlation coefficient (PCC). The graph shows the mean PCC from three independent biological repeats, in each of which at least 10 randomly selected fields of view per condition were analysed. Error bars are mean±s.d., **P*<0.05 and n.s. indicates that the difference between conditions is not significant as determined using the multiple comparisons function within the ordinary one-way ANOVA statistical test, followed by a Dunnett *post hoc* test, when comparing to non-targeting siRNA-treated control condition.

Journal of Cell Science (2018) 131, jcs211342. doi:10.1242/jcs.211342

Upon retromer depletion, or abrogation of retromer interaction with a transmembrane cargo, that cargo molecule will not recycle through the endosomal network effectively. Often this results in decreased whole cell levels of the cargo in question, due to leakage of that protein into the lysosomal degradative pathway (Temkin et al., 2011; Steinberg et al., 2013; Gallon et al., 2014). We observed that whole cell levels of PC2 are decreased upon suppression of VPS35 in HeLa cells, and found that, as expected, GLUT1 levels fell following VPS35 knockdown. (Fig. 8Ai-iii). In ADPKD, loss of PC2 results in defective ciliary targeting of PC1; indeed, PC2 has even been described as a molecular chaperone for PC1 (Kim et al., 2014; Gainullin et al., 2015). If retromer is regulating PC2 recycling, we would expect ciliary levels of PC1 to fall upon depletion of VPS35. As knockdown of VPS35 is likely to disrupt myriad intracellular trafficking pathways that might affect PC1 localisation, we sought to test whether disruption of the PC2-retromer interaction affects ciliary localisation of PC1 in a targeted manner. We therefore transiently expressed PC2 constructs bearing mutations in the region required for association with retromer (p.I54A and p.I59A), in addition to PC2-p.R7AxP9A (AxA) as a negative control, in *PKD2*-knockout kidney tubule cells. As expected (Su et al., 2015), we found that

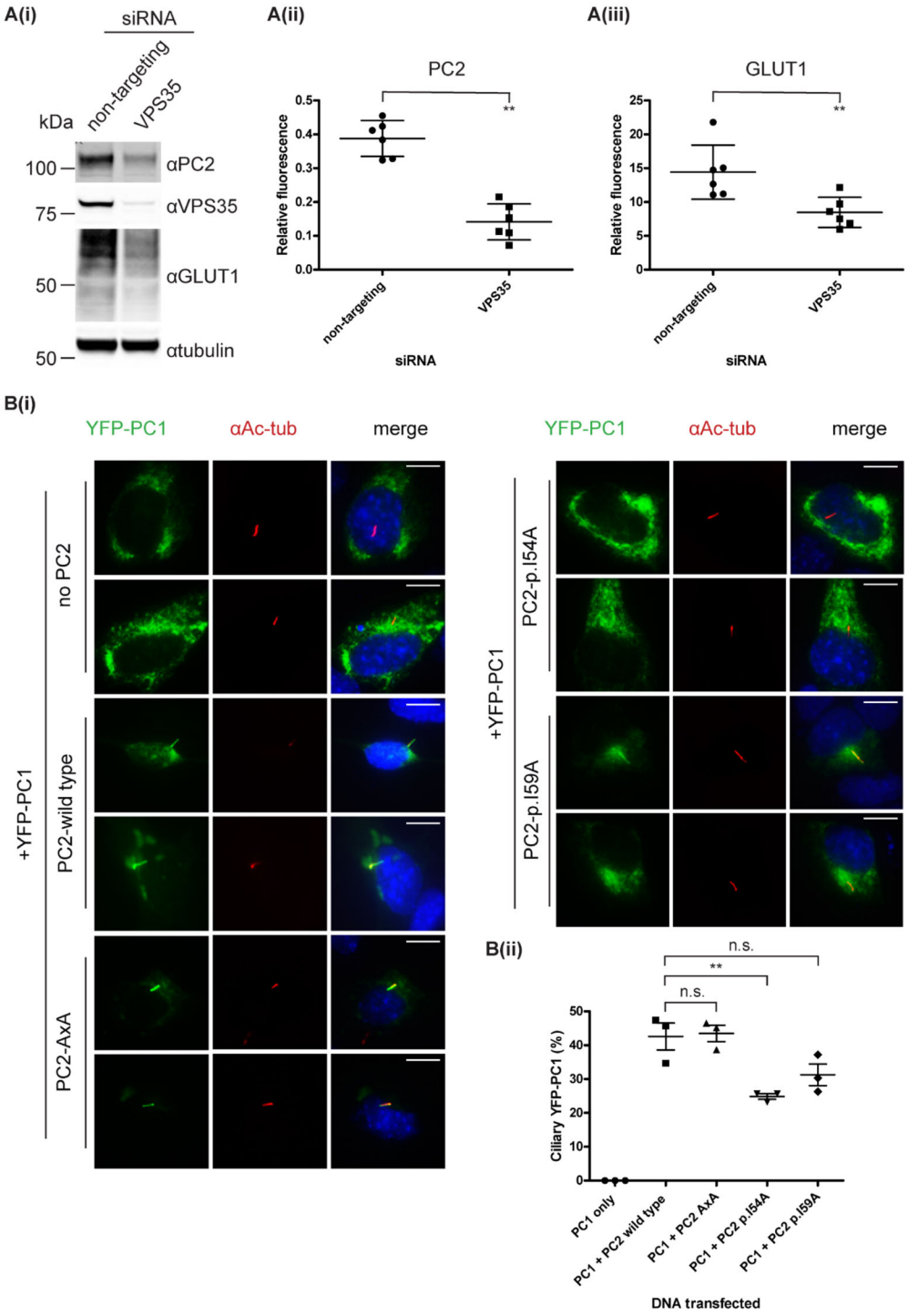

Fig. 8. Ciliary targeting of PC1 is reduced with expression of PC2 p.I54A and PC2 p.I59A-myc. (Ai) Western blot showing the effect of VPS35 suppression on whole cell levels of PC2 and GLUT1. (Aii,iii) PC2 and GLUT1 levels in VPS35-suppressed cells were quantified using an Odyssey infrared scanner (LI-COR). Graph shows the relative fluorescence intensity from six biological repeats. Error bars are s.d., $^{**}P<0.01$ compared with control condition as determined using an unpaired two-tailed Student's *t*-test. (Bi) Fluorescence imaging of *PKD2*-knockout mouse kidney tubule cells transiently expressing YFP-PC1 and the indicated PC2 constructs, stained for acetylated tubulin (Ac-tub) to mark the primary cilium. YFP-PC1 was visualised using an anti-GFP antibody. Scale bar: 5 µm. (Bii) Efficiency of PC1 cilia localisation, defined as the number of cells with YFP-PC1-positive cilium divided by the total number of YFP-PC1-transfected cells that possess a primary cilium. Graph shows the average PC1 trafficking efficiency from three independent biological repeats, in each of which at least 100 cells per condition were quantified. Error bars are mean ±s.d., $^{**}P<0.01$ and n.s. indicates that difference between conditions is not significant as determined using the multiple comparisons function within the ordinary one-way ANOVA statistical test followed by a Dunnett *post hoc* test, compared with the wild-type PC1-PC2 condition.

Journal of Cell Science (2018) 131, jcs211342. doi:10.1242/jcs.211342

PC1 is entirely absent from the primary cilia of *PKD2*-knockout cells. Reintroduction of wild-type PC2, or PC2 bearing the p.R7AxP9A mutation, partially rescues the PC1 trafficking defect. We observed that although PC1 is capable of being trafficked to the primary cilium of cells expressing PC2 p.I54A and PC2 p.I59A-myc, this amount was reduced to a significant extent in GFP-PC2 p.I54A cells, and showed a trend to decrease in cells expressing PC2 p.I59A-myc when compared with cells expressing wild-type PC2 or PC2-AxA (Fig. 8Bi,ii).

DISCUSSION

Based on our data that demonstrate PC2 preferentially immunoprecipitates retromer when its C-terminal ER-retention site is either deleted or occluded by PC1 binding, that PC2 protein levels fall following VPS35 suppression in our cell system, and that ciliary levels of PC1 are decreased in *PKD2*-knockout kidney tubule cells expressing PC2 constructs bearing mutations in the region required for association with retromer, we propose that PC2 may be a retromer cargo molecule. In this scenario, retromer would associate with PC2 that has been internalised either from the bulk plasma membrane or from the cilium base, and delivers PC2 either directly back to the plasma membrane, or to compartments of the biosynthetic trafficking network, where it may associate with PC1 and undergo further rounds of ciliary targeting.

Our alanine scan screen has revealed a retromer-association motif in the N-terminus of PC2, with the sequence [G-x-x-I-E-M-Q-x-I-x]. This sequence, comprising amino acids with a mixture of hydrophobic and hydrophilic properties, bears no similarity to known retromer-binding motifs (Seaman, 2004; Fjorback et al., 2012), and to our knowledge, is not shared with any other transmembrane proteins. Interpretation of the importance of various amino acids within this region for retromer association was hampered by the fact that in this study, we were not able to demonstrate direct binding of the PC2 N-terminal domain to retromer subunits in isolation. Based on our observation that PC2 is capable of retromer-independent association with the WASH complex, and that an atypical Parkinsonian-associated variant of VPS26A, p.K297X, exhibits increased association with PC2 compared to wild-type VPS26A (McMillan et al., 2016) (Fig. S2A), we have hypothesised that PC2 is binding retromer through multivalent interactions, for example, at the interface of two or more retromer subunits, or retromer and a retromer-associated protein. As VPS26 p.K297X lacks the site required for interaction with SNX27, we initially hypothesised that under physiological conditions, binding of SNX27 to retromer limits the ability of PC2 to associate with the complex, perhaps by creating steric hindrance around VPS26A. However, we have found that suppression of SNX27 does not increase the association of GFP-VPS26A with PC2 (Fig. S2B). We have consistently observed the most robust immunoprecipitation of PC2 with the VPS35 retromer subunit. Although the VPS35 interaction site on VPS26A, found between residues Ile235 and Ile246 (Shi et al., 2006), is not precisely adjacent to the site of premature truncation in VPS26A p.K297X, it is not unreasonable to suppose that deletion of the region encompassing residues Lys297-Met327 in VPS26A modifies architecture of the retromer heterotrimer in such a way that promotes increased binding to PC2, perhaps by increasing availability of a binding surface or pocket in VPS35. We suppose that a similar mechanism of binding is occurring between retromer and the recently identified retromer-interacting protein DENND4C, a Rab10 guanine exchange factor that also exhibits increased binding to VPS26A p.K297X compared with wild-type VPS26A (Yoshimura et al., 2010; McMillan et al., 2016) (Fig. S2A). As there exists no sequence similarity between the region in DENND4C and PC2 required for association with retromer (data not shown), it seems likely that architecture of the retromer complex as a whole affects interaction with both these proteins. In fact, while our manuscript was in preparation, it was demonstrated through the use of a tri-cistronic vector encoding VPS26, VPS29 and VPS35, that PC2 does indeed directly bind the retromer complex (Feng et al., 2017). In addition, this study established the interaction of endogenous PC2 with endogenous VPS35, and interestingly reported increased levels of PC2 and PC1 at the bulk plasma membrane following retromer depletion. Although the study of Feng and colleagues did not include analysis of ciliary PC1 levels upon retromer knockdown (Feng et al., 2017), given that PC2 exists in complex with PC1 at the primary cilium, this result is in contrast to our finding that ciliary levels of PC1 are decreased in *PKD*-knockout cells re-expressing PC2 p.I54A and p.I59A-myc. That said, it may be that the cell types used in this and our study have different trafficking requirements, and rely on the retromer complex to different extents for the internalisation and retrograde trafficking of polycystin proteins.

Surprisingly, the recently published retromer interactome, in which PC2 was originally identified as a putative retromer-binding protein, is entirely devoid of established retromer cargo proteins. Sortilin (Seaman, 2007), SORLA (Fjorback et al., 2012), Wntless (Harterink et al., 2011; Zhang et al., 2011) and the divalent metal transporter-1 (DMT1) (Tabuchi et al., 2010) do not bind retromer or a retromer-associated protein with sufficient affinity to enable detection by immunoprecipitation followed by mass spectrometry. Cargo molecules that associate with retromer indirectly, such as GLUT1, the copper transporter ATP7A (Menkes protein) (Steinberg et al., 2013) and the β2-AR (Lauffer et al., 2010; Temkin et al., 2011) were also entirely absent. Our data give some indication that PC2 may be a retromer cargo molecule, yet the fact that PC2 is the only transmembrane protein identified in the core retromer interactome is intriguing, as it suggests that PC2 is capable of binding retromer, or a retromer-associated protein, with an affinity much greater than that of any known retromer cargoes. Most of the proteins contained within the core retromer interactome have regulatory functions within the endosomal recycling network; TBC1D5 for example, is a GTPase-activating protein for Rab7, which regulates recruitment of retromer to the endosome membrane (Seaman et al., 2009; Harrison et al., 2014). Similarly, DNAJC13 (RME-8) participates in the maintenance of endosome subdomains (Shi et al., 2009; Freeman et al., 2014), and the interaction between ANKRD27 (VARP) and retromer has been proposed to regulate Rab-GTPase switching to control cargo export from endosomes (Zhang et al., 2006; Hesketh et al., 2014; McGough et al., 2014). Although we have observed that PC2 does not regulate the ability of retromer to recycle GLUT1, perhaps PC2 possesses a different, as yet undefined function within the endosomal network. As the predominant subcellular localisation of PC2 is the ER (Koulen et al., 2002), and we have demonstrated that it is the cytoplasmic N-terminal domain of PC2 that possesses ability to associate with retromer, we hypothesised that endosome-localised VPS35 may interact with ER-bound PC2, potentially constituting an endosome-ER contact site. Functions for the abundant ER-endosome contacts that form as endosomes traffic and mature include regulation of endosome positioning and cholesterol sensing (Rocha et al., 2009; Rowland et al., 2014), phosphoinositide transfer (Dong et al., 2016), as well as transfer of calcium ions (Ca^{2+}) (Phillips and Voeltz, 2016). The luminal Ca^{2+}

Journal of Cell Science (2018) 131, jcs211342. doi:10.1242/jcs.211342

concentration of endosomes increases with maturation (Albrecht et al., 2015), and it has recently been demonstrated that the ER, and specifically, the ER-resident inositol-1,4,5-trisphosphate receptor (IP_3R), is responsible for refilling lysosomes with Ca^{2+} (Garrity et al., 2016). Interestingly, the C-terminal domain of PC2 may physically interact with the IP_3R, with the function of extending the half-life of IP_3-induced Ca^{2+} spikes (Li et al., 2005; Santoso et al., 2011). In addition, binding of the soluble NSF attachment protector receptor (SNARE) protein syntaxin-5 to PC2 is known to negatively regulate PC2 channel activity (Geng et al., 2008). As the syntaxin-5 binding site in PC2 overlaps with the region required for retromer association, it would be interesting to determine whether syntaxin-5 and retromer compete for PC2 binding, whether these proteins have opposing effects in terms of regulation of PC2 channel activity, and any potential consequences of retromer binding to PC2 in terms of IP_3R activity and local calcium ion concentration around the endosome. We acknowledge that the hypothesis that PC2 may function to regulate endosomal Ca^{2+} concentration is highly speculative, but believe this theory to be supported by a recent study demonstrating involvement of PC1 and PC2 in promoting mitochondrial uptake of Ca^{2+} from the ER (Padovano et al., 2017).

MATERIALS AND METHODS

Antibodies

Primary antibodies used in this study were rabbit polyclonal VPS35 (Abcam, ab97545; IF, 1:200), rabbit monoclonal VPS35 [Abcam, ab157220, clone EPR11501(B); WB, 1:2000], rabbit polyclonal VPS26A (Abcam, ab137447; WB, 1:1000), rabbit polyclonal VPS26B (Proteintech, 15915-1-AP; WB, 1:250), rabbit polyclonal VPS29 (Abcam, ab98929; WB, 1:500), mouse monoclonal GFP (Roche, 11814460001, clone 7.1 and 13.1; WB, 1:2000), rabbit polyclonal GFP (used for YFP staining) (Abcam, ab290; IF, 1:20,000), mouse monoclonal SNX1 (BD Transduction, 611482, clone 51/SNX1; IF, 1:100), mouse monoclonal SNX27 (Abcam, ab77799, clone IC6; WB, 1:500), rabbit polyclonal strumpellin (Santa Cruz Biotechnology, 87442; WB, 1:500), mouse monoclonal tubulin (Sigma-Aldrich, T9026, clone DM1A, WB: 1/5000), rabbit polyclonal PC2 (Santa Cruz Biotechnology, sc-25749; WB, 1:250), mouse monoclonal acetylated tubulin (Sigma-Aldrich, T6793, clone 6-11B-1; IF, 1:100,000), mouse monoclonal mCherry (Abcam, ab125096, clone IC51; WB, 1:2000), rabbit monoclonal GLUT1 (Abcam, ab115730; IF, 1:500), mouse monoclonal LAMP1 (Developmental Studies Hybridoma Bank, 1DB4; IF, 1:500), rabbit polyclonal DENND4C (Sigma-Aldrich, HPA014917; WB, 1:250), mouse monoclonal myc (AbD Serotec, MCA2200, clone 7E12; WB, 1:2000), mouse monoclonal GST (Santa Cruz, sc-138, clone B-14; WB, 1:1000), mouse monoclonal His (Sigma-Aldrich, H1029, clone HIS-1; IF, 1:1000), and rabbit polyclonal FAM21 (a gift from Daniel D. Billadeau, Mayo Clinic, Rochester, MN; WB, 1:1000).

Plasmids

N-terminal [PC2-(1-48), PC2-(1-60), PC2-(1-70), PC2-(1-84), PC2-(1-94), PC2-(1-156) and PC2-(1-223)] and C-terminal [PC2-(680-968)] fragments of PC2 were subcloned into either pEGFP-N1 or pEGFP-C1 from an original plasmid containing full-length PC2, which was a gift from Stefan Somlo (Yale Nephrology, New Haven, CT). Primers for these reactions are listed in Table S1. Site-directed mutagenesis was used to introduce the point mutations p.R6G, p.V7A, p.P9A, p.E48A, p.Q49A, p.R50A, p.G51A, p.L52A, p.E53A, p.I54A, p.E55A, p.M56A, p.Q57A, p.R58A, p.I59A and p.R60A into PC2 (1-223-GFP), and the p.I54A and p.I59A mutations into full-length PC2 and PC2-myc, using the primers listed in Table S2. PC2 (1-703-GFP) was cloned from HeLa cDNA into a pEGFP-N1 vector using the primers also indicated in Table S1. Mouse PC2-GFP was generated, and the p.R7AxP9A mutation introduced, as previously described (Su et al., 2015). FAM21(1-356) was subcloned into pEGFPC1 from an original full-length FAM21-containing plasmid, which was a gift from Daniel D. Billadeau (Mayo Clinic, Rochester, MN), and is initially described in Steinberg et al. (2013). YFP-PC1 was generated by inserting YFP immediately downstream of the PC1 signal peptide as previously described (Su et al., 2014). mCherry-PC1 was a gift from Peter C. Harris (Mayo Clinic, Rochester, MN). mCherry-SNX1 was cloned as described in Hunt et al. (2013).

Production of lentivirally transduced RPE-1 cells and PKD2-knockout kidney tubule cells

Lentivirally transduced RPE-1 cells were produced as described previously (McMillan et al., 2016). *Pkd2*-knockout kidney tubule cells were generated by isolating kidney tubule cells from the PKD2-knockout mouse using the marker DBA, followed by immortalisation with a temperature-sensitive SV40 construct.

Cell culture and DNA transfection

HEK293T (from ATCC, cat. no. CRL-3216), hTERT RPE-1 (from ATCC, CRL-4000) and HeLa (from ATCC, cat no. CCL-2) cells were cultured in DMEM (Sigma, D5796), supplemented with 10% (v/v) fetal bovine serum (FBS) (HEK293T and RPE-1: Sigma, F7524; HeLa: Gibco, 10270098) at 37°C, 5% CO_2. *PKD2*-knockout kidney tubule cells were routinely cultured at 33°C, 5% CO_2 in DMEM/F12 (50:50) (Corning cell grow, 10-090-CV) supplemented with 10% FBS (Gibco, 10437-028) and 5 U/ml interferon-gamma (Sigma, I4777) HeLa cells were transiently transfected with PC2 peptide constructs at 50-70% confluence using FuGENE-HD (Promega, E2311) and Opti-MEM (Gibco, 31985062) according to the manufacturer's instructions. HEK293T cells were transiently transfected at 80-90% confluence with various constructs using 25 kDa linear PEI (polyethylenimine, Polysciences, 23966-2) and Opti-MEM. Cells were processed for biochemistry or imaging either 24 or 48 h following transfection, depending on the nature of the DNA transfected. For PC1 trafficking assays in *PKD2*-knockout cells, cells were transiently transfected at 70-80% confluence with PC2 and PC1 constructs using PEI and MEM medium (Mediatech, MT10010CV). After 24 h, cells were moved to a 37°C incubator and serum starved in DMEM/F12 2% FCS with interferon-gamma withdrawal for 36 h before processing for imaging experiments.

siRNA

For both FAM21C and SNX27 suppression, cells were transfected with a mixture of four ON-TARGETplus siRNA oligos (Dharmacon, GE Healthcare, LQ-0296678-01 and L-017346-01). For VPS35 suppression, cells were transfected with a mixture of two ON-TARGETplus oligos (Dharmacon, GE Healthcare, J-010894-07 and J-010894-08). Cells were typically treated twice with targeting siRNA in order to achieve adequate knockdown. In all knockdown experiments, cells treated with a non-targeting siRNA with the sequence (5′-gacaagaaccagaacgcca[dTdT]-3′) were also included as a negative control. siRNA transfections were carried out using DharmaFECT1 (GE Healthcare, T-2001) and Opti-MEM with GlutaMAX supplement (Gibco, 51985034). Cells were processed for biochemistry or imaging either 72 or 96 h following the first siRNA transfection. In order to assess levels of protein knockdown, cells were lysed in an appropriate volume of PBS-based lysis buffer (PBS pH7.4, 5 mM EDTA, 1% Triton X-100 and complete protease inhibitor cocktail) and protein concentration determined using BCA assay. Protein extracts were then analysed by standard western blotting procedures.

Immunofluorescence

For fluorescence microscopy, cells which had been plated onto glass coverslips were first fixed in 4% (v/v) paraformaldehyde in phosphate-buffered saline (PBS) for 20 min before being washed three times in PBS. The second wash was supplemented with 30 mM glycine. Cells were then permeabilised for 5 min in PBS 0.1% (v/v) Triton X-100, washed a further three times in PBS and then blocked in PBS 1% (w/v) bovine serum albumin (BSA) for 1 h at room temperature. Cells were then incubated in primary antibodies diluted in PBS 1% (w/v) BSA, also for 1 h at room temperature. After a further 3× PBS washes, cells were incubated in fluorescently-conjugated secondary antibodies (Molecular Probes) diluted 1/400 in PBS 1% (w/v) BSA for 1 h at room temperature. After a final two washes in PBS and one in distilled water, coverslips were mounted onto microscope

slides using Fluoromount-G (eBioscience, 00–4958-02). If one of the proteins to be stained was LAMP1, then cells were permeabilised in PBS with 0.1% (w/v) saponin (Sigma-Aldrich, 47036), and all subsequent washing and staining steps were carried out in the presence of 0.01% (w/v) saponin.

Live cell imaging

For live cell imaging, cells expressing fluorescently tagged proteins were plated onto glass-bottomed MatTEK dishes. Before imaging, growth medium was removed and replaced with pre-warmed CO_2-independent medium (Gibco, 18045-054). Cells were then moved to a Leica SP8 AOBS confocal microscope attached to a Leica DM I6000 inverted epifluorescence microscope, and imaged at 37°C for the required amount of time.

GFP, mCherry and myc immunoisolation and western blot analysis

To immunoprecipitate proteins labelled with GFP, mCherry or myc tags, cells expressing these constructs, either transiently or lentivirally, were lysed in a Tris-based immunoprecipitation buffer [20 mM Tris-HCl, pH 7.4, 0.5% (v/v) Igepal plus complete protease inhibitor cocktail (Roche, 04693124001)]. Lysates were cleared by centrifugation at 14,000 ***g*** for 10 min at 4°C and then incubated with either GFP-trap (Chromotek, gta-20), RFP-trap (Chromotek, rta-20) or myc-trap (Pierce, 20168) beads for 1 h at 4°C. These beads were then washed and proteins eluted by resuspension in 2× LDS-sample buffer (NuPAGE, NP0007) supplemented with 2.5% (v/v) β-mercaptoethanol. Western blotting was then performed using standard procedures. Fluorescently labelled secondary antibodies (Life Technologies) were detected using an Odyssey Fc imaging system from LI-COR Biosciences (Cambridge, UK). HRP-conjugated secondary antibodies (Jackson ImmunoResearch) were detected by exposing the membrane to Hyperfilm (GE Healthcare, 8-9068-37), which was then developed using an AGFA Curix 60 machine.

Production of recombinant proteins

For purification of GST-tagged and His-tagged proteins, BL-21 cells (Stratagene) were transformed with protein expression plasmids, and grown to an OD600 of 0.6 in Luria-Bertani (LB) broth at 37°C. Protein expression was induced by the addition of isopropyl β-D-1-thiogalactopyranoside (IPTG) to a final concentration of 0.1 mM. The bacteria were then grown overnight at 15°C, before being pelleted by centrifugation at 4000 ***g*** for 15 min. Pellets were resuspended in lysis buffer [PBS with 1% (v/v) Triton X-100 plus 1× complete protease inhibitor cocktail, pH 7.4] and disrupted by pulse sonication (3× for 30 s at the highest frequency). The lysates were cleared by centrifugation at 16,000 ***g*** for 60 min at 4°C. Glutathione-Sepharose beads (Generon) were used to purify GST-tagged proteins, and HIS-Select Cobalt Affinity Gel (Sigma, H8162) was used to purify His-tagged proteins. Beads were first washed in 20 mM HEPES, 150 mM NaCl, 2 mM EDTA, 2 mM DTT, pH 7.4 (for GST-tag) or 50 mM Tris, 150 mM NaCl, 10 mM imidazole, pH 8.0 (for His-tag), and then incubated with the bacterial lysate for 2 h at 4°C with rotation. Beads were then again washed three times in the appropriate buffer. Where required, proteins were eluted from the beads by overnight incubation at 4°C with either PreScission protease (GE Healthcare, 27-083-01) (for GST-tagged proteins) or 50 mM Tris-HCl, 150 mM NaCl, 100 mM imidazole, pH 8.0 (for His-tagged proteins), followed by centrifugation at 4000 ***g*** for 2 min and removal of the resulting supernatant.

Image acquisition and subsequent analysis

Confocal images were captured using either a Leica SP5II or SP8 laser scanning microscope attached to a Leica DMI 6000 inverted epifluorescence microscope, equipped with either a 63× or 100× oil immersion objective (numerical aperture: 1.4). Microscope settings were kept constant across different conditions in the same experiment. Pearson's correlation coefficient (PCC) was used as an indicator of colocalisation between different fluorescence channels. These values were obtained using the colocalisation tool within Volocity 6.3 software (PerkinElmer), after a uniform threshold had been applied to filter noise. For PC1 trafficking assays, cells were analysed using a Nikon-1000 epifluorescence microscope. To determine the PC1 ciliary localisation efficiency, the number of ciliated YFP-PC1-positive cells in randomly selected microscope fields was divided by the total number of YFP-PC1-transfected cells that also possessed a primary cilium

Sequence alignment

The length of the PC2 N-terminal domain amino acid sequence in different species was determined using the domain boundaries proposed in the UniProt database (www.uniprot.org). Sequences were aligned using the Qiagen CLC Sequence Viewer 7.7.1 (Aarhus, Denmark).

Statistical analysis

Statistical analyses were carried out using GraphPad Prism 7 software (La Jolla, CA). Either an ordinary one-way ANOVA followed by Dunnett's *post hoc* test or an unpaired Student's *t*-test were used to determine whether differences between conditions were statistically significant (defined as such if $P<0.05$).

Acknowledgements

We would like to thank past and current members of the Cullen lab for useful discussions and help with experiments, and Drs Daniel D. Billadeau, Peter C. Harris and Stefan Somlo for reagents.

Competing interests

The authors declare no competing or financial interests.

Author contributions

Conceptualization: F.C.T., J.Z., P.J.C.; Methodology: F.C.T., J.Z., P.J.C.; Validation: F.C.T., M.G., C.L., C.M.D.; Formal analysis: F.C.T., M.G., C.L., C.M.D.; Investigation: F.C.T., M.G., C.L., C.M.D.; Resources: M.G., C.L., C.M.D.; Writing - original draft: F.C.T., J.Z., P.J.C.; Writing - review & editing: F.C.T., J.Z., P.J.C.; Visualization: F.C.T., M.G., C.L., C.M.D., J.Z.; Supervision: J.Z., P.J.C.; Funding acquisition: J.Z., P.J.C.

Funding

F.C.T. was supported by a studentship funded through the Wellcome Trust Dynamic Cell Biology PhD programme (089928). Research in the Cullen lab is supported by grants awarded through the Wellcome Trust (104568/Z/14/Z) and the Medical Research Council (MR/L007363/1 and MR/P018807/1). C.L. was supported by funding from National Natural Science Foundation of China (2012AA02A512). Research in the Zhou lab is supported by grants from the National Institutes of Health (RO1DK099532) and the U.S. Department of Defense (W81XWH-16-1-0617) to J.Z. Deposited in PMC for release after 6 months.

Supplementary information

Supplementary information available online at
http://jcs.biologists.org/lookup/doi/10.1242/jcs.211342.supplemental

References

Albrecht, T., Zhao, Y., Nguyen, T. H., Campbell, R. E. and Johnson, J. D. (2015). Fluorescent biosensors illuminate calcium levels within defined beta-cell endosome subpopulations. *Cell Calcium* **57**, 263-274.

Bhattacharyya, S., Rainey, M. A., Arya, P., Dutta, S., George, M., Storck, M. D., Mccomb, R. D., Muirhead, D., Todd, G. L., Gould, K. et al. (2016). Endocytic recycling protein EHD1 regulates primary cilia morphogenesis and SHH signaling during neural tube development. *Sci. Rep.* **6**, 20727.

Cai, Y., Fedeles, S. V., Dong, K., Anyatonwu, G., Onoe, T., Mitobe, M., Gao, J.-D., Okuhara, D., Tian, X., Gallagher, A.-R. et al. (2014). Altered trafficking and stability of polycystins underlie polycystic kidney disease. *J. Clin. Invest.* **124**, 5129-5144.

Casuscelli, J., Schmidt, S., Degray, B., Petri, E. T., ?elić, A., Folta-Stogniew, E., Ehrlich, B. E. and Boggon, T. J. (2009). Analysis of the cytoplasmic interaction between polycystin-1 and polycystin-2. *Am. J. Physiol. Renal Physiol.* **297**, F1310-F1315.

Chapin, H. C. and Caplan, M. J. (2010). The cell biology of polycystic kidney disease. *J. Cell Biol.* **191**, 701-710.

Dong, R., Saheki, Y., Swarup, S., Lucast, L., Harper, J. W. and De Camilli, P. (2016). Endosome-ER contacts control actin nucleation and retromer function through VAP-dependent regulation of PI4P. *Cell* **166**, 408-423.

Fedeles, S. V., Gallagher, A.-R. and Somlo, S. (2014). Polycystin-1: a master regulator of intersecting cystic pathways. *Trends Mol. Med.* **20**, 251-260.

Feng, S., Streets, A. J., Nesin, V., Tran, U., Nie, H., Onopiuk, M., Wessely, O., Tsiokas, L. and Ong, A. C. M. (2017). The sorting nexin-3 retromer pathway

regulates the cell surface localization and activity of a Wnt-Activated polycystin channel complex. *J. Am. Soc. Nephrol.* **28**, 2973-2984.
Fjorback, A. W., Seaman, M., Gustafsen, C., Mehmedbasic, A., Gokool, S., Wu, C., Militz, D., Schmidt, V., Madsen, P., Nyengaard, J. R. et al. (2012). Retromer binds the FANSHY sorting motif in SorLA to regulate amyloid precursor protein sorting and processing. *J. Neurosci.* **32**, 1467-1480.
Fogelgren, B., Lin, S.-Y., Zuo, X., Jaffe, K. M., Park, K. M., Reichert, R. J., Bell, P. D., Burdine, R. D. and Lipschutz, J. H. (2011). The exocyst protein Sec10 interacts with Polycystin-2 and knockdown causes PKD-phenotypes. *PLoS Genet.* **7**, e1001361.
Freeman, C. L., Hesketh, G. and Seaman, M. N. J. (2014). RME-8 coordinates the activity of the WASH complex with the function of the retromer SNX dimer to control endosomal tubulation. *J. Cell Sci.* **127**, 2053-2070.
Gainullin, V. G., Hopp, K., Ward, C. J., Hommerding, C. J. and Harris, P. C. (2015). Polycystin-1 maturation requires polycystin-2 in a dose-dependent manner. *J. Clin. Invest.* **125**, 607-620.
Gallon, M. and Cullen, P. J. (2015). Retromer and sorting nexins in endosomal sorting. *Biochem. Soc. Trans.* **43**, 33-47.
Gallon, M., Clairfeuille, T., Steinberg, F., Mas, C., Ghai, R., Sessions, R. B., Teasdale, R. D., Collins, B. M. and Cullen, P. J. (2014). A unique PDZ domain and arrestin-like fold interaction reveals mechanistic details of endocytic recycling by SNX27-retromer. *Proc. Natl. Acad. Sci. USA* **111**, E3604-E3613.
Garrity, A. G., Wang, W., Collier, C. M. D., Levey, S. A., Gao, Q. and Xu, H. (2016). The endoplasmic reticulum, not the pH gradient, drives calcium refilling of lysosomes. *eLife* **5**, e15887.
Geng, L., Okuhara, D., Yu, Z., Tian, X., Cai, Y., Shibazaki, S. and Somlo, S. (2006). Polycystin-2 traffics to cilia independently of polycystin-1 by using an N-terminal RVxP motif. *J. Cell Sci.* **119**, 1383-1395.
Geng, L., Boehmerle, W., Maeda, Y., Okuhara, D. Y., Tian, X., Yu, Z., Choe, C., Anyatonwu, G. I., Ehrlich, B. E. and Somlo, S. (2008). Syntaxin 5 regulates the endoplasmic reticulum channel-release properties of polycystin-2. *Proc. Natl. Acad. Sci. USA* **105**, 15920-15925.
Hanaoka, K., Qian, F., Boletta, A., Bhunia, A. K., Piontek, K., Tsiokas, L., Sukhatme, V. P., Guggino, W. B. and Germino, G. G. (2000). Co-assembly of polycystin-1 and -2 produces unique cation-permeable currents. *Nature* **408**, 990-994.
Harbour, M. E., Breusegem, S. Y. A., Antrobus, R., Freeman, C., Reid, E. and Seaman, M. N. J. (2010). The cargo-selective retromer complex is a recruiting hub for protein complexes that regulate endosomal tubule dynamics. *J. Cell Sci.* **123**, 3703-3717.
Harbour, M. E., Breusegem, S. Y. and Seaman, M. N. J. (2012). Recruitment of the endosomal WASH complex is mediated by the extended 'tail' of Fam21 binding to the retromer protein Vps35. *Biochem. J.* **442**, 209-220.
Harrison, M. S., Hung, C.-S., Liu, T.-T., Christiano, R., Walther, T. C. and Burd, C. G. (2014). A mechanism for retromer endosomal coat complex assembly with cargo. *Proc. Natl. Acad. Sci. USA* **111**, 267-272.
Harterink, M., Port, F., Lorenowicz, M. J., Mcgough, I. J., Silhankova, M., Betist, M. C., Van Weering, J. R. T., Van Heesbeen, R. G. H. P., Middelkoop, T. C., Basler, K. et al. (2011). A SNX3-dependent retromer pathway mediates retrograde transport of the Wnt sorting receptor Wntless and is required for Wnt secretion. *Nat. Cell Biol.* **13**, 914-923.
Hesketh, G. G., Pérez-Dorado, I., Jackson, L. P., Wartosch, L., Schäfer, I. B., Gray, S. R., McCoy, A. J., Zeldin, O. B., Garman, E. F., Harbour, M. E. et al. (2014). VARP Is recruited on to endosomes by direct interaction with retromer, where together they function in export to the cell surface. *Dev. Cell* **29**, 591-606.
Hunt, S. D., Townley, A. K., Danson, C. M., Cullen, P. J. and Stephens, D. J. (2013). Microtubule motors mediate endosomal sorting by maintaining functional domain organization. *J. Cell Sci.* **126**, 2493-2501.
Jia, D., Gomez, T. S., Billadeau, D. D. and Rosen, M. K. (2012). Multiple repeat elements within the FAM21 tail link the WASH actin regulatory complex to the retromer. *Mol. Boil. Cell* **23**, 2352-2361.
Kim, H., Xu, H., Yao, Q., Li, W., Huang, Q., Outeda, P., Cebotaru, V., Chiaravalli, M., Boletta, A., Piontek, K. et al. (2014). Ciliary membrane proteins traffic through the Golgi via a Rabep1/GGA1/Arl3-dependent mechanism. *Nat. Commun.* **5**, 5482.
Köttgen, M., Benzing, T., Simmen, T., Tauber, R., Buchholz, B., Feliciangeli, S., Huber, T. B., Schermer, B., Kramer-Zucker, A., Höpker, K. et al. (2005). Trafficking of TRPP2 by PACS proteins represents a novel mechanism of ion channel regulation. *EMBO J.* **24**, 705-716.
Koulen, P., Cai, Y., Geng, L., Maeda, Y., Nishimura, S., Witzgall, R., Ehrlich, B. E. and Somlo, S. (2002). Polycystin-2 is an intracellular calcium release channel. *Nat. Cell Biol.* **4**, 191-197.
Koumandou, V. L., Klute, M. J., Herman, E. K., Nunez-Miguel, R., Dacks, J. B. and Field, M. C. (2011). Evolutionary reconstruction of the retromer complex and its function in Trypanosoma brucei. *J. Cell Sci.* **124**, 1496-1509.
Lauffer, B. E. L., Melero, C., Temkin, P., Lei, C., Hong, W., Kortemme, T. and Von Zastrow, M. (2010). SNX27 mediates PDZ-directed sorting from endosomes to the plasma membrane. *J. Cell Biol.* **190**, 565-574.
Lee, S., Chang, J. and Blackstone, C. (2016). FAM21 directs SNX27-retromer cargoes to the plasma membrane by preventing transport to the Golgi apparatus. *Nat. Commun.* **7**, 10939.
Li, Y., Wright, J. M., Qian, F., Germino, G. G. and Guggino, W. B. (2005). Polycystin 2 interacts with type I inositol 1,4,5-trisphosphate receptor to modulate intracellular Ca2+ signaling. *J. Biol. Chem.* **280**, 41298-41306.
Lu, Q., Insinna, C., Ott, C., Stauffer, J., Pintado, P. A., Rahajeng, J., Baxa, U., Walia, V., Cuenca, A., Hwang, Y.-S. et al. (2015). Early steps in primary cilium assembly require EHD1/EHD3-dependent ciliary vesicle formation. *Nat. Cell Biol.* **17**, 228-240.
Ma, M., Tian, X., Igarashi, P., Pazour, G. J. and Somlo, S. (2013). Loss of cilia suppresses cyst growth in genetic models of autosomal dominant polycystic kidney disease. *Nat. Genet.* **45**, 1004-1012.
Mcgough, I. J., Steinberg, F., Gallon, M., Yatsu, A., Ohbayashi, N., Heesom, K. J., Fukuda, M. and Cullen, P. J. (2014). Identification of molecular heterogeneity in SNX27-retromer-mediated endosome-to-plasma-membrane recycling. *J. Cell Sci.* **127**, 4940-4953.
McMillan, K. J., Gallon, M., Jellett, A. P., Clairfeuille, T., Tilley, F. C., Mcgough, I. J., Danson, C. M., Heesom, K. J., Wilkinson, K. A., Collins, B. M. et al. (2016). Atypical parkinsonism-associated retromer mutant alters endosomal sorting of specific cargo proteins. *J. Cell Biol.* **214**, 389-399.
Naslavsky, N. and Caplan, S. (2011). EHD proteins: key conductors of endocytic transport. *Trends Cell Biol.* **21**, 122-131.
Nauli, S. M., Alenghat, F. J., Luo, Y., Williams, E., Vassilev, P., Li, X., Elia, A. E. H., Lu, W., Brown, E. M., Quinn, S. J. et al. (2003). Polycystins 1 and 2 mediate mechanosensation in the primary cilium of kidney cells. *Nat. Genet.* **33**, 129-137.
Nauli, S. M., Rossetti, S., Kolb, R. J., Alenghat, F. J., Consugar, M. B., Harris, P. C., Ingber, D. E., Loghman-Adham, M. and Zhou, J. (2006). Loss of polycystin-1 in human cyst-lining epithelia leads to ciliary dysfunction. *J. Am. Soc. Nephrol.* **17**, 1015-1025.
Nothwehr, S. F., Bruinsma, P. and Strawn, L. A. (1999). Distinct domains within Vps35p mediate the retrieval of two different cargo proteins from the yeast prevacuolar/endosomal compartment. *Mol. Biol. Cell* **10**, 875-890.
Novick, P., Field, C. and Schekman, R. (1980). Identification of 23 complementation groups required for post-translational events in the yeast secretory pathway. *Cell* **21**, 205-215.
Padovano, V., Kuo, I. Y., Stavola, L. K., Aerni, H. R., Flaherty, B. J., Chapin, H. C., Ma, M., Somlo, S., Boletta, A., Ehrlich, B. E. et al. (2017). The polycystins are modulated by cellular oxygen-sensing pathways and regulate mitochondrial function. *Mol. Biol. Cell* **28**, 261-269.
Phillips, M. J. and Voeltz, G. K. (2016). Structure and function of ER membrane contact sites with other organelles. *Nat. Rev. Mol. Cell Biol.* **17**, 69-82.
Rocha, N., Kuijl, C., Van Der Kant, R., Janssen, L., Houben, D., Janssen, H., Zwart, W. and Neefjes, J. (2009). Cholesterol sensor ORP1L contacts the ER protein VAP to control Rab7-RILP-p150 Glued and late endosome positioning. *J. Cell Biol.* **185**, 1209-1225.
Rojas, R., Kametaka, S., Haft, C. R. and Bonifacino, J. S. (2007). Interchangeable but essential functions of SNX1 and SNX2 in the association of retromer with endosomes and the trafficking of mannose 6-phosphate receptors. *Mol. Cell. Biol.* **27**, 1112-1124.
Rossetti, S., Consugar, M. B., Chapman, A. B., Torres, V. E., Guay-Woodford, L. M., Grantham, J. J., Bennett, W. M., Meyers, C. M., Walker, D. L., Bae, K. et al. (2007). Comprehensive molecular diagnostics in autosomal dominant polycystic kidney disease. *J. Am. Soc. Nephrol.* **18**, 2143-2160.
Rowland, A. A., Chitwood, P. J., Phillips, M. J. and Voeltz, G. K. (2014). ER contact sites define the position and timing of endosome fission. *Cell* **159**, 1027-1041.
Santoso, N. G., Cebotaru, L. and Guggino, W. B. (2011). Polycystin-1, 2, and STIM1 interact with IP_3R to modulate ER Ca^{2+} release through the PI3K/Akt Pathway. *Cell. Physiol. Biochem.* **27**, 715-726.
Seaman, M. N. J. (2004). Cargo-selective endosomal sorting for retrieval to the Golgi requires retromer. *J. Cell Biol.* **165**, 111-122.
Seaman, M. N. J. (2007). Identification of a novel conserved sorting motif required for retromer-mediated endosome-to-TGN retrieval. *J. Cell Sci.* **120**, 2378-2389.
Seaman, M. N. J., Mccaffery, J. M. and Emr, S. D. (1998). A membrane coat complex essential for endosome-to-Golgi retrograde transport in yeast. *J. Cell Biol.* **142**, 665-681.
Seaman, M. N. J., Harbour, M. E., Tattersall, D., Read, E. and Bright, N. (2009). Membrane recruitment of the cargo-selective retromer subcomplex is catalysed by the small GTPase Rab7 and inhibited by the Rab-GAP TBC1D5. *J. Cell Sci.* **122**, 2371-2382.
Shi, H., Rojas, R., Bonifacino, J. S. and Hurley, J. H. (2006). The retromer subunit Vps26 has an arrestin fold and binds Vps35 through its C-terminal domain. *Nat. Struct. Mol. Biol.* **13**, 540-548.
Shi, A., Sun, L., Banerjee, R., Tobin, M., Zhang, Y. and Grant, B. D. (2009). Regulation of endosomal clathrin and retromer-mediated endosome to Golgi retrograde transport by the J-domain protein RME-8. *EMBO J.* **28**, 3290-3302.
Steinberg, F., Gallon, M., Winfield, M., Thomas, E. C., Bell, A. J., Heesom, K. J., Tavaré, J. M. and Cullen, P. J. (2013). A global analysis of SNX27-retromer

assembly and cargo specificity reveals a function in glucose and metal ion transport. *Nat. Cell Biol.* **15**, 461-471.
Su, X., Driscoll, K., Yao, G., Raed, A., Wu, M., Beales, P. L. and Zhou, J. (2014). Bardet-Biedl syndrome proteins 1 and 3 regulate the ciliary trafficking of polycystic kidney disease 1 protein. *Hum. Mol. Genet.* **23**, 5441-5451.
Su, X., Wu, M., Yao, G., El-Jouni, W., Luo, C., Tabari, A. and Zhou, J. (2015). Regulation of polycystin-1 ciliary trafficking by motifs at its C-terminus and polycystin-2 but not by cleavage at the GPS site. *J. Cell Sci.* **128**, 4063-4073.
Sung, C.-H. and Leroux, M. R. (2013). The roles of evolutionarily conserved functional modules in cilia-related trafficking. *Nat. Cell Biol.* **15**, 1387-1397.
Tabuchi, M., Yanatori, I., Kawai, Y. and Kishi, F. (2010). Retromer-mediated direct sorting is required for proper endosomal recycling of the mammalian iron transporter DMT1. *J. Cell Sci.* **123**, 756-766.
Temkin, P., Lauffer, B., Jäger, S., Cimermancic, P., Krogan, N. J. and Von Zastrow, M. (2011). SNX27 mediates retromer tubule entry and endosome-to-plasma membrane trafficking of signalling receptors. *Nat. Cell Biol.* **13**, 715-721.
Terbush, D. R., Maurice, T., Roth, D. and Novick, P. (1996). The Exocyst is a multiprotein complex required for exocytosis in Saccharomyces cerevisiae. *EMBO J.* **15**, 6483-6494.
Torres, V. E., Harris, P. C. and Pirson, Y. (2007). Autosomal dominant polycystic kidney disease. *Lancet* **369**, 1287-1301.
Xu, Y., Streets, A. J., Hounslow, A. M., Tran, U., Jean-Alphonse, F., Needham, A. J., Vilardaga, J.-P., Wessely, O., Williamson, M. P. and Ong, A. C. M. (2016). The polycystin-1, lipoxygenase, and alpha-toxin domain regulates polycystin-1 trafficking. *J. Am. Soc. Nephrol.* **27**, 1159-1173.
Yoder, B. K., Hou, X. and Guay-Woodford, L. M. (2002). The polycystic kidney disease proteins, polycystin-1, polycystin-2, polaris, and cystin, are co-localized in renal cilia. *J. Am. Soc. Nephrol.* **13**, 2508-2516.
Yoshimura, S., Gerondopoulos, A., Linford, A., Rigden, D. J. and Barr, F. A. (2010). Family-wide characterization of the DENN domain Rab GDP-GTP exchange factors. *J. Cell Biol.* **191**, 367-381.
Yu, F., Sharma, S., Skowronek, A. and Erdmann, K. S. (2016). The serologically defined colon cancer antigen-3 (SDCCAG3) is involved in the regulation of ciliogenesis. *Sci. Rep.* **6**, 35399.
Zhang, X., He, X., Fu, X.-Y. and Chang, Z. (2006). Varp is a Rab21 guanine nucleotide exchange factor and regulates endosome dynamics. *J. Cell Sci.* **119**, 1053-1062.
Zhang, P., Wu, Y., Belenkaya, T. Y. and Lin, X. (2011). SNX3 controls Wingless/Wnt secretion through regulating retromer-dependent recycling of Wntless. *Cell Res.* **21**, 1677-1690.
Zhou, J. (2009). Polycystins and primary cilia: primers for cell cycle progression. *Ann. Rev. Physiol.* **71**, 83-113.
Zhou, J. and Pollak, M. (2015). Polycystic kidney disease and other inherited tubular disorders. (ed. D. Kasper, A. Fauci, S. Hauser, D. Longo, J. L. Jameson, J. Loscalzo), pp. 813-814. New York: McGraw-Hill; 2015.